ISSN (Print) : 2320 – 3765
ISSN (Online): 2278 – 8875

International Journal of Advanced Research in Electrical, Electronics and Instrumentation Engineering

(An ISO 3297: 2007 Certified Organization)

Website: www.ijareeie.com

Vol. 6, Issue 7, July 2017

Performance Analysis of Spectral Angle Mapper and Spectral Information Divergence Classifiers; A Case Study using Homogeneous and Heterogeneous Remotely Sensed Data

S.V.Rajashekararadhya[1], Shivakumar.B.R[2]

Professor, Dept. of ECE, Kalpataru Institute of Technology, Tiptur, India[1]

Assistant Professor, Dept. of ECE, NMAM Institute of Technology, Nitte, India[2]

ABSTRACT:The concept of remote sensing is to study the properties of Earth's objects by recording its reflection. Development in remote sensing has been consistent in the past few decades ranging from optical to microwave domains. Classification is the process of extracting information about the characteristics of the objects present on the Earth's surface. Selection of suitable classification algorithm is dependent on the environmental conditions and the distribution of land units. An attempt has been made to classify coastal agro-climatic zone IRS-p6/LISS III and arid agro-climatic zone Landsat-8 data sets using two spectral classifiers: Spectral Angle Mapper (SAM) and Spectral Information Divergence (SID) classifiers. Accuracy assessment was performed to study the potential of the classifiers. The results of the classifiers has been analysed with respect to the spectral characteristics of the data sets. This study analyses the effect of spectral overlapping on classification accuracy. Homogenous data set produced higher accuracy values for all classifiers considered.

KEYWORDS: Remote Sensing, Classification, Spectral Angle Mapper, Spectral Information Divergence.

I.INTRODUCTION

In the field of remote sensing image analysis and pattern recognition, image classification plays an important part in extracting information from the imagery. In many cases, the process of classification itself can be the object of analysis where the classifier output is a map like image. Hence, for the examination of digital images, image classification may be considered as an important tool. Remotely sensed images can be of multiple types including multispectral, hyperspectral, panchromatic and ultraspectral. The process of classification is dependent on a lot of data parameters like spectral overlapping, presence of one or more types of noise, and the algorithm used.

Homogeneous data are said to have clear boundaries between its Land Use Land Cover (LULC) classes. This enables the classifiers to assign pixels to their corresponding classes with less mismatch. Heterogeneous data sets are complex in their LULC distribution over the Earth surface and cause mixed pixels [1][2]. Mixed pixels are said to lie over the boundaries of two or more LULC classes. These pixels represent a part of two or more LULC classes. An example of mixed pixels can be pictured as when a forest transitions from an evergreen to deciduous, there is no abrupt boundary between the two forests. The transition zone of these two classes pose a challenge to classification. Hard classifiers find it difficult to classify these mixed pixels as the information content in a transition zone belongs to more than one LULC classes [3][4].

Classification is broadly categorized into hard and soft classifiers. Hard classifiers use traditional Boolean logic to assign a pixel to a class. They assume that a pixel may completely represent a class or completely not represent it. These classifiers find it difficult to differentiate between pure pixels and mixed pixels [3][4]. Pure pixels are those which very strongly represent a LULC class. Hard classifiers may be used for classifying homogeneous data and still

ISSN (Print) : 2320 – 3765
ISSN (Online): 2278 – 8875

International Journal of Advanced Research in Electrical, Electronics and Instrumentation Engineering

(An ISO 3297: 2007 Certified Organization)

Website: www.ijareeie.com

Vol. 6, Issue 7, July 2017

obtain respectable results. Soft or Fuzzy classifiers use Fuzzy logic to find the percentage of spectral content of a pixel to all LULC classes defined while training, and assign the pixel to the class to which the pixel shows highest similarity.

The objective of this study is to analyse the performance of selected spectral classifiers over homogeneous and heterogeneous terrain conditions. The study also aims at finding the dependency of the selected classifiers over a certain type of data (homogeneous or heterogeneous) to produce expected results. Also, the study intends to find the dependency of the selected classifiers over the spatial resolution and number of LULC classes defined in the data.

The rest of the paper is presented as follows. In section 2, the study areas considered for experimentation are presented. Section 3 presents the data and classification methods involved in the study. Section 4 discusses the results obtained by the experiment. Section 5 derives useful conclusions from the experimentation results.

II.STUDY AREA

This study considers two agro-climatic zones as study areas: Coastal agro-climatic zone and arid agro-climatic zone. This section provides brief introduction to the study areas.

A. Coastal Zone Data

The coastal agro-climatic zone data considered is a multispectral (4 dimensional) data. The spatial resolution of this data is 23.5m. The selected rectangular geographical area is located between the points N 140 37′ 38′ E 740 18′ 01″ and N 140 23′ 32″ E 740 31′ 28′ as shown in Fig. 1 and lies in Kumta Taluk, North Canara District, India. It is a part of coastal agro-climatic region mainly covering natural vegetation including evergreen forest. It also covers part of Western Ghats with continuous undulated terrain. The data also contains a shore line that separates Arabic ocean from Indian subcontinent. The aim of the study was to classify this RS imagery into 8 land-use land-cover (LU/LC) classes: i. Deep Sea Water ii. Shallow Sea Water iii. River Water iv. Evergreen Forest v. Kharif vi. Scrub Land vii. Salt Mines and vii. Submerged Land.

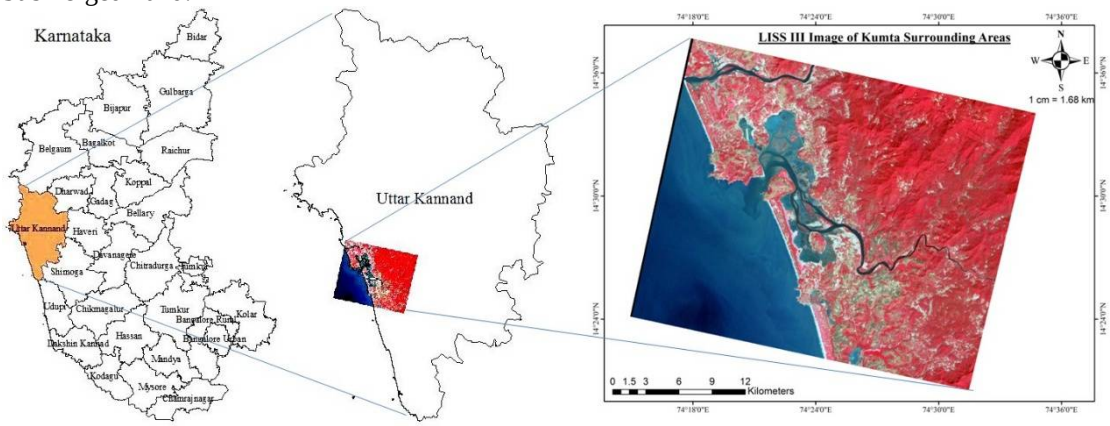

Fig. 1. Coastal zone IRS-P6/LISS III study area.

B. Arid Zone Data

The arid agro-climatic zone data is a multispectral LANDSAT-8 imagery (7 dimensional). It has a spatial resolution of 15m.The selected rectangular geographical area is located between the points N 17^0 35′ 53″ E 76^0 28′ 08″ and N 16^0 57′ 25″ E 77^0 18′ 12″ as in Fig. 2. It is located in Gulbarga District, Karnataka, India. It is a part of arid agro-climatic region which normally is a flat land with less undulated terrain and high wind speed. It majorly covers agricultural lands and has less natural vegetation cover. The objective of using this image was to classify the land units into seven land-use land-cover classes: i. Kharif ii. Double Crop iii. Water Body iv. Built-Up v. Dense Thicket vi. Barren Land and vi. Scrub Land.

ISSN (Print) : 2320 – 3765
ISSN (Online): 2278 – 8875

International Journal of Advanced Research in Electrical, Electronics and Instrumentation Engineering

(An ISO 3297: 2007 Certified Organization)

Website: www.ijareeie.com

Vol. 6, Issue 7, July 2017

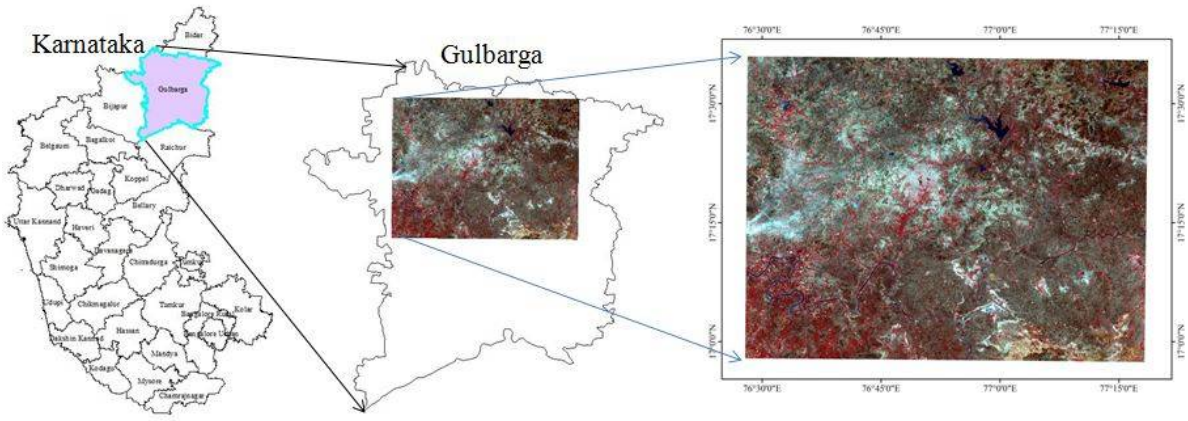

Fig. 2. Arid zone Landsat-8 study area (Data courtesy USGS [5]).

III. DATA AND CLASSIFICATION METHODS

Selection of remote sensing data for monitoring land-use land-cover is a complex step as it affects the accuracy and correctness of the results [6]. For validating the classifiers, two data sets were considered in this paper: IRS-p6/LISS III data and LANDSAT 8 data.

A. IRS-P6/LISS III Data

IRS-p6 Linear Imaging Self Scanning III (LISS III) image was accessed by Indian Remote Sensing (IRS) p6 platform. It consists of 4 spectral bands: Green (0.52-0.59 µm), Red (0.62-0.68 µm), Near Infrared (NIR) (0.77-0.86 µm), and short wave infrared (SWIR) (1.55-1.70 µm) bands with a spatial resolution of 23.5m. It was acquired on 24th of January 2006 and is free from clouds and aerosols. The data did not have spatial reference and so it was georectified to World Geodetic System (WGS) 1984. The prepared data can be useful for studying land information by processing appropriate algorithms.

B. Landsat-8 Data

Land Satellite 8 (Landsat-8) data was accessed by U.S. Geological Survey. It consists of 11 spectral bands, of which this study makes use of the first 8 bands: Coastal Aerosol (0.43-0.45µm), Blue (0.45-0.51 µm), Green (0.53-0.59 µm), Red (0.64-0.67 µm), Near Infrared (NIR) (0.85-0.88 µm), Short-Wave Infrared-1 (SWIR 1) (1.57-1.65 µm), Short-Wave Infrared-2 (SWIR 2) (2.11-2.29 µm), and Panchromatic (0.50-0.68 µm)[7]. Spatial resolution of first seven bands is 30m and that of Panchromatic is 15m. This data was acquired on 25thofMarch 2015, which is pre-summer season and it is free from clouds although a small part of the data is slightly covered by haze.

C. Spectral Angle Mapper(SAM) Classifier

SAM classifier considers spectral angle,α, to establish the spectral similarity between an image pixel spectrumt and the training or reference pixel spectrum rin an n-dimensional feature space, where nis the number of available spectral bands [8][9][10][11][12][13] .

$$\alpha = arccos\left(\frac{\sum_{i=1}^{n} t_i r_i}{\sum_{i=1}^{n} t_i \sum_{i=1}^{n} r_i}\right) \quad (1)$$

where, t_i is test spectrum, r_i is reference spectrum.

The reference spectra may be obtained either from laboratory or from field measurements or directly from the image. SAM estimates the spectral similarity between test and reference spectra treating them as vectors in the n-dimensional

ISSN (Print) : 2320 – 3765
ISSN (Online): 2278 – 8875

International Journal of Advanced Research in Electrical, Electronics and Instrumentation Engineering

(An ISO 3297: 2007 Certified Organization)

Website: www.ijareeie.com

Vol. 6, Issue 7, July 2017

space [14][15][10]. The estimated spectral angle is independent of the vectors length which makes SAM immune to solar illumination effects. One of the most advantageous things of SAM is its ability to rapidly map the spectral similarity of image spectra to reference spectra. It also represses the influence of shading effects to accentuate the target reflectance characteristics [13].

D. Spectral Information Divergence (SID)Classifier

SID is a spectral classification method that makes use of divergence measure to match pixels to reference spectra. The lesser the divergence, the more probable the pixels are similar [16]. A threshold can be placed to mapping the pixels. Pixels that have greater divergence compared to the threshold are not classified [17]. Unlike SAM classifier which calculates the spectral angle between two spectra, each pixel spectrum in SID is considered as a random variable and the divergence of probabilistic behaviours between the two spectral vectors is measured [18].

$$SID(A,B) = D(A||B) + D(B||A) \quad (2)$$

where,

$$D(A||B) = -\sum_{i=1}^{N} p_i \log(p_i/q_i) \quad (3)$$

$$D(B||A) = -\sum_{i=1}^{N} q_i \log(q_i/p_i) \quad (4)$$

$$p_i = \frac{A_i}{\sum_{i=1}^{N} A_i} \quad (5)$$

$$q_i = \frac{B_i}{\sum_{i=1}^{N} B_i} \quad (6)$$

where, N refers to the number of bands, and $A = (A_1,A_2,...,A_N)$ and $B = (B_1,B_2,...,B_N)$ refer to the two spectral vectors, respectively. Here, the lower the SID value, the higher the similarity of both spectral vectors.

IV. RESULT AND DISCUSSION

A. SID Classifier Resultsfor IRS-P6/LISS III data

Fig. 3 indicates the SID classified image for the IRS-p6 LISS III data set. Evergreen Forest class was effectively classified with a Kappa coefficient of 1 (PA =88.25%, UA = 100%). Shallow Sea Water (PA = 90.74%, UA = 98.00%) and DeepSea Water (PA = 72.73%, UA = 88.89%) classes were also well extracted with a Kappa coefficient of 0.9704 and 0.8782 respectively. SID classifier extracted Kharif (PA = 85.9%, UA = 72.83%) and Submerged Land (PA = 69.23%, UA = 69.23%) with decent accuracy values. River Water, Scrub Land, and Submerged Land classes were found to be poorly extracted by SID classifier. No ground points were generated for salt mines by the stratified random points generator, and hence salt mines class did not yield accuracy results. Results of SID for IRS-P6/LISS III data are shown in TABLE 1.

TABLE 1. Results of SID classification for coastal study area.

Class Name	Reference Totals	Classified Totals	Number Correct	Producer's Accuracy	Omission Error	User's Accuracy	Commission Error	Kappa Value (k_{hat})
Deep Sea Water	44	36	32	72.73%	27.27 %	88.89%	11.11 %	0.8782
Shallow Sea Water	162	150	147	90.74%	09.26 %	98.00%	02.00 %	0.9704
River Water	21	45	16	76.19%	23.81 %	35.56%	64.44 %	0.3273
Evergreen Forest	170	150	150	88.25%	11.75 %	100.00%	00.00 %	1.0000
Kharif	78	92	67	85.90%	14.1 %	72.83%	27.17 %	0.6780
Scrub Land	11	5	1	9.09%	90.91 %	20.00%	80.00 %	0.182
Salt Mine	1	9	0	00.00%	100.00 %	00.00%	100.00 %	-0.002
Submerged Land	13	13	9	69.23%	30.77 %	69.23%	30.77 %	0.6841
Total	500	500	422					
Overall Classification Accuracy				**(422/500)*100 = 84.40 %**				
Overall Kappa Statistic				**0.7950**				

ISSN (Print) : 2320 – 3765
ISSN (Online): 2278 – 8875

International Journal of Advanced Research in Electrical, Electronics and Instrumentation Engineering

(An ISO 3297: 2007 Certified Organization)

Website: www.ijareeie.com

Vol. 6, Issue 7, July 2017

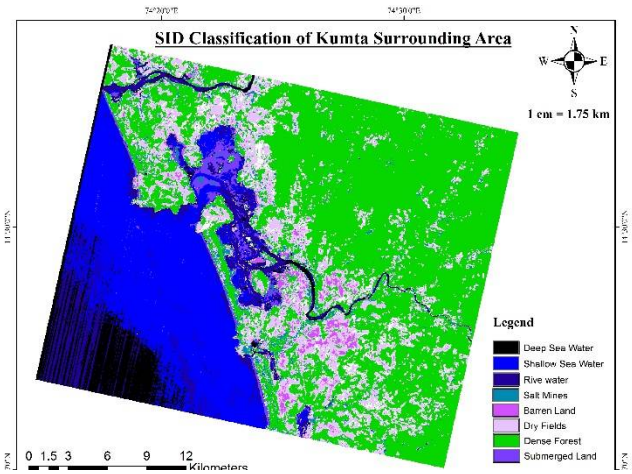

Fig. 3. SID classified map of coastal zone data.

B. SID ClassifierResults for LANDSAT-8 data

Fig. 4 shows the SID classified image for the LANDSAT-8 data set. TABLE 2 shows the results of SID for LANDSAT-8 data. Kharif (PA = 48.06%, UA = 100%) and Water Body (PA = 100.00%, UA = 100%) classes were effectively classified with a Kappa coefficient of 1. Double Crop (PA = 70.83%, UA = 60.71%) and Barren Land (PA = 77.78%, UA= 66.67%) classes were classified with average accuracies. Built Up, Dense Thicket, and Scrub Land classes were classified with poor accuracy values.

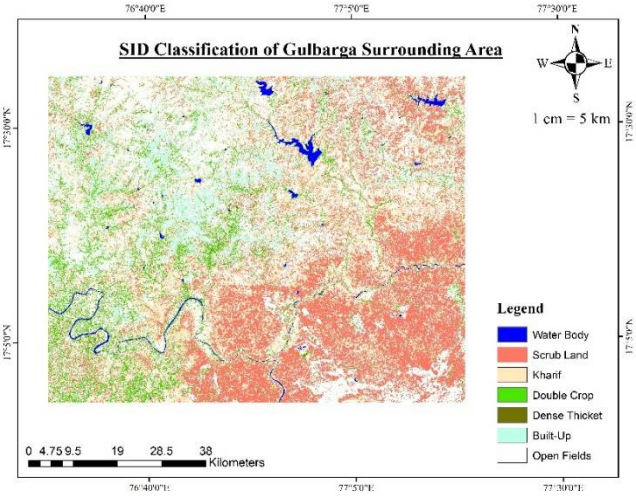

Fig. 4. SID classified map of arid zone data.

C. SAM Classifier Results for IRS-P6/LISS III data

Fig. 5 shows the Spectral Angle Mapper classified image. Once again, Evergreen Forest class was found to be the best extracted class with a Kappa coefficient of 1 (PA = 85.60%, UA = 100%), closely followed by Shallow Sea Water (PA = 92.77%, UA = 96.25%), and Deep Sea Water (PA = 100%, UA = 95.71%). Unlike SID, SAM classifier successfully extracts all of the remaining classes with average accuracy values. TABLE 3 shows the results of SAM for IRS-P6/LISS III data.

ISSN (Print) : 2320 – 3765
ISSN (Online): 2278 – 8875

International Journal of Advanced Research in Electrical, Electronics and Instrumentation Engineering

(An ISO 3297: 2007 Certified Organization)

Website: www.ijareeie.com

Vol. 6, Issue 7, July 2017

TABLE 2. Results of SID classification for Arid study area.

Class Name	Reference Totals	Classified Totals	Number Correct	Producer's Accuracy	Omission Error	User's Accuracy	Commission Error	Kappa Value (k_{hat})
Kharif	129	62	62	48.06 %	51.94 %	100.00 %	00.00 %	1.0000
Double Crop	24	28	17	70.83 %	29.17 %	60.71 %	39.29 %	0.5654
Water Body	8	8	8	100.00 %	00.00 %	100.00 %	00.00 %	1.0000
Built Up	10	34	7	70.00 %	30.00 %	20.59 %	79.41 %	0.1728
Dense Thicket	12	2	1	8.33 %	91.67 %	50.00 %	50.00 %	0.4748
Barren Land	18	21	14	77.78 %	22.22 %	66.67 %	33.33 %	0.6408
Scrub Land	49	95	43	87.76 %	12.24 %	45.26 %	54.74 %	0.3192
Total	250	250	152					
Overall Classification Accuracy				**(152/250)*100 = 60.80%**				
Overall Kappa Statistic				**0.4935**				

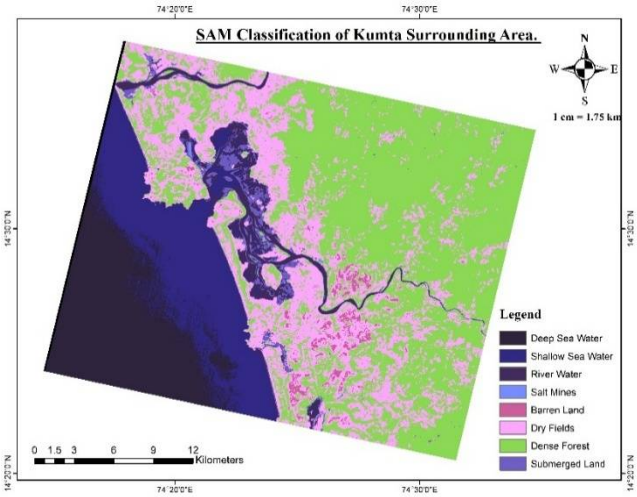

Fig. 5. SAM classified map of coastal zone data.

TABLE 3. Results of SAM classification for Coastal study area.

Class Name	Reference Totals	Classified Totals	Number Correct	Producer's Accuracy	Omission Error	User's Accuracy	Commission Error	Kappa Value (k_{hat})
Deep Sea Water	67	36	32	72.73 %	27.27 %	88.89 %	11.11 %	0.8782
Shallow Sea Water	83	150	147	90.74 %	09.26 %	98.00 %	02.00 %	0.9704
River Water	18	45	16	76.19 %	23.81 %	35.56 %	64.44 %	0.3273
Evergreen Forest	243	150	150	88.25 %	11.75 %	100.00 %	00.00 %	1.0000
Kharif	74	92	67	85.90 %	14.10 %	72.83 %	27.17 %	0.6780
Scrub Land	6	5	1	9.09 %	90.91 %	20.00 %	80.00 %	0.182
Salt Mine	1	9	0	00.00 %	100.00 %	00.00 %	100.00 %	-0.002
Submerged Land	8	13	9	69.23 %	30.77 %	69.23 %		0.6841
Total	500	500	422					
Overall Classification Accuracy				**(422/500)*100 = 84.40%**				
Overall Kappa Statistic				**0.7950**				

D. SAM Classifier Results for LANDSAT-8 data

Fig. 6 shows the Spectral Angle Mapper classified image for LANDSAT-8 imagery. Among the seven classes considered for LANDSAT-8 data, Kharif (PA = 70.95%, UA = 91.30%) and Water Body (PA = 100.00%, UA = 95.24%) classes were accurately classified with kappa values of 0.7869 and 0.9482 respectively. SAM classified Double Crop (PA = 38.10%, UA = 72.73%) and Barren Land (PA = 71.45%, UA = 62.50%) with reasonable accuracy values. SAM extracted Built Up (PA = 63.64%, UA = 31.11%) class with a low accuracy. TABLE 4 shows the results of SAM for LANDSAT-8 data.

ISSN (Print) : 2320 – 3765
ISSN (Online): 2278 – 8875

International Journal of Advanced Research in Electrical, Electronics and Instrumentation Engineering

(An ISO 3297: 2007 Certified Organization)

Website: www.ijareeie.com

Vol. 6, Issue 7, July 2017

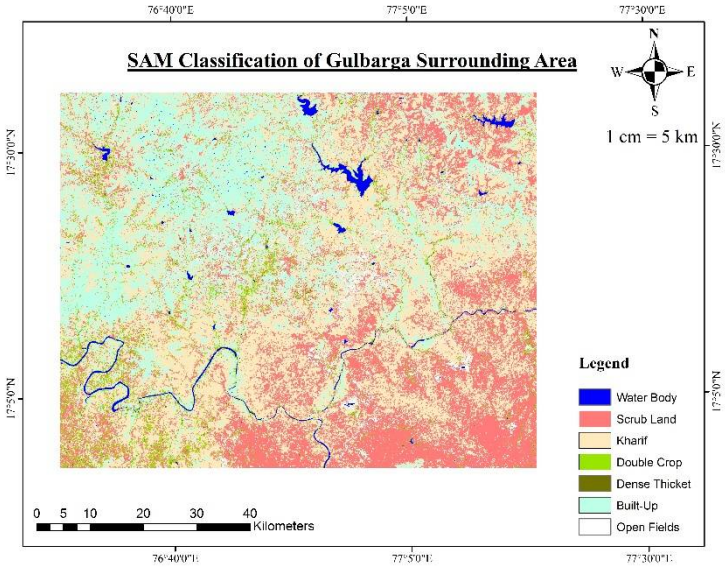

Fig. 6. SAM classified map of arid zone data.

TABLE 4. Results of SAM classification for Arid study area.

Class Name	Reference Totals	Classified Totals	Number Correct	Producer's Accuracy	Omission Error	User's Accuracy	Commission Error	Kappa Value (k_{hat})
Kharif	148	115	105	70.95	29.05	91.30	08.70	0.7869
Double Crop	21	11	8	38.10	61.9	72.73	27.27	0.7023
Water Body	20	21	20	100.00	00.00	95.24	04.76	0.9482
Built Up	22	45	14	63.64	36.36	31.11	68.89	0.2446
Dense Thicket	9	6	3	33.33	66.67	50.00	50.00	0.4813
Barren Land	7	8	5	71.45	28.55	62.50	37.50	0.6142
Scrub Land	23	44	22	95.65	4.35	50.00	50.00	0.4493
Total	250	250	177					
Overall Classification Accuracy				**70.80%**				
Overall Kappa Statistic				**0.5728**				

V.CONCLUSION

The availability of Remotely Sensed data, coupled with the computer software necessary to analyse it, provides opportunities for environmental scholars and planners, particularly in the areas of land use mapping and change detection that would have been unheard of only a few decades ago. Both the classifiers fared well while extracting information from IRS-p6/LISS III imagery. However, the classifiers found it very hard to efficiently extract information from a heterogeneous data. Hence, it can be stated that addition of extra bands do not increase the accuracy of classification. Also, presence of aerosols in the LANDSAT-8 data affected the accuracy values as most of Built Up class pixels were misclassified because of the presence of aerosol. SAM classifier produced better results than SID classifier for both the study areas considered. Hence, it can also be stated that SAM classifier is computationally more efficient than SID classifier. Also, another important observation is that, the considered classifiers produced a considerable lesser number of misclassifications while classifying homogeneous data. Hence, it can be concluded that increase in spatial resolution does not necessarily increase the classification accuracy. The resultsare accurate for the local environment conditions and the results may vary as the nature of the data changes.

REFERENCES

[1] J. R. Jensen, *Introductory digital image processing: a remote sensing perspective*, 3rd ed. New Jersey: Prentice-Hall Inc., 2000.
[2] J. A. Richards, *Remote Sensing Digital Image Analysis- An Introduction*, 5th ed. Springer, 2006.

ISSN (Print) : 2320 – 3765
ISSN (Online): 2278 – 8875

International Journal of Advanced Research in Electrical, Electronics and Instrumentation Engineering

(An ISO 3297: 2007 Certified Organization)

Website: www.ijareeie.com

Vol. 6, Issue 7, July 2017

[3] B. R. Shivakumar and S. V. Rajashekararadhya, "Spectral Similarity for Evaluating Classification Performance of Traditional Classifiers," in *International Conference on Wireless Communications Signal Processing and Networking*, 2017, pp. 2028–2033.

[4] B. R. Shivakumar and S. V. Rajashekararadhya, "Performance Evaluation of Spectral Angle Mapper and Spectral Correlation Mapper Classifiers over Multiple Remote Sensor Data," in *2017 Second IEEE International Conference on Electrical, Computer and Communication Technologies*, 2017, pp. 677–684.

[5] USGS, "Earthexplorer." [Online]. Available: https://earthexplorer.usgs.gov/. [Accessed: 01-Jan-2017].

[6] D. Duan, Y. Shi, L. Sun, and G. Wang, "Remote sensing technology's applied research and development direction in Land-Use and Land-Cover Change (LUCC)," *2012 2nd Int. Conf. Remote Sensing, Environ. Transp. Eng. RSETE 2012 - Proc.*, pp. 12–15, 2012.

[7] K. Zanter, "Landsat 8 (L8) Data Users Handbook," *LSDS-1574 Version*, vol. 2.0, no. 1993, 2016.

[8] A. F. H. G. F.A. Kruse, A.B. Lefkoff, J.W. Boardman, K.B. Heidebrecht, A.T. Shapiro, P.J. Barloon, "The Spectral Image Processing System (SIPS) - Interactive Visualization and Analysis of Imaging Spectrometer Data," *Remote Sens. Environ.*, vol. 44, no. 2–3, pp. 145–163, 1993.

[9] R. H. Yuhas, F. H. Goetz, and J. W. Boardman, "Discrimination Among Semi-Arid Landscape Endmembers Using The Spectral Angle Mapper Algorithm," *Summ. 3rd Annu. JPL Airborne Geosci. Work.*, pp. 147–149, 1992.

[10] F. VanderMeer, M. Vazquez-Torres, and P. M. Van Dijk, "Spectral characterization of ophiolite lithologies in the Troodos Ophiolite complex of Cyprus and its potential in prospecting for massive sulphide deposits," *Int. J. Remote Sens.*, vol. 18, no. 6, pp. 1245–1257, 1997.

[11] J. Schwarz and K. Staenz, "Adaptive threshold for spectral matching of hyperspectral data," *Can. J. Remote Sens.*, vol. 27, no. 3, pp. 216–224, 2001.

[12] E. Hunter and C. Power, "An assessment of two classification methods for mapping Thames Estuary intertidal habitats using CASI data," *Int. J. Remote Sens.*, vol. 23, no. 15, pp. 2989–3008, 2002.

[13] O. A. de Carvalho Jr and P. R. Meneses, "Spectral Correlation Mapper (SCM): An Improvement on the Spectral Angle Mapper (SAM)," *Summ. 9th JPL Airborne Earth Sci. Work. JPL Publ. 00-18*, vol. 9, 2000.

[14] F. Kruse *et al.*, "The spectral image processing system (SIPS)-interactive visualization and analysis of imaging spectrometer data," *Remote Sens. Environ.*, vol. 44, no. 2–3, pp. 145–163, 1993.

[15] L. C. Rowan and J. C. Mars, "Lithologic mapping in the Mountain Pass, California area using Advanced Spaceborne Thermal Emission and Reflection Radiometer (ASTER) data," *Remote Sens. Environ.*, vol. 84, no. 3, pp. 350–366, 2003.

[16] C. Chang, "Spectral Information Divergence for Hyperspectral Image Analysis," *IEEE 1999 Int. Geosci. Remote Sens. Symp. Vol. 1*, no. 1, pp. 509–511, 1999.

[17] M. Khaleghi, H. Ranjbar, J. Shahabpour, and M. Honarmand, "Spectral angle mapping, spectral information divergence, and principal component analysis of the ASTER SWIR data for exploration of porphyry copper mineralization in the Sarduiyeh area, Kerman province, Iran," *Appl. Geomatics*, vol. 6, no. 1, pp. 49–58, 2014.

[18] D. Ma *et al.*, "Spectral similarity assessment based on a spectrum reflectance-absorption index and simplified curve patterns for hyperspectral remote sensing," *Sensors (Switzerland)*, vol. 16, no. 2, 2016.